

# Synthesis of periodic mesoporous organosilica from bis(triethoxysilyl)methane and their pyrolytic conversion into porous SiCO glasses

Bérangère Toury, Florence Babonneau\*

*Chimie de la Matière Condensée—Université Paris 6/CNRS, 4 place Jussieu, 75252 Paris cedex 05, France*

Available online 12 October 2004

## Abstract

Periodic mesoporous organosilica (PMO) have been prepared from bis(triethoxysilyl)methane (BTM) and cetyltrimethylammonium chloride ( $C_{16}$ TAC). A large range of synthesis conditions (pH,  $C_{16}$ TAC/BTM ratio, post-treatment and concentration) were used to study their effects on the structure of the as-prepared meso-structured samples. The sample obtained with the optimised composition presents a 2D-hexagonal structure with a large surface area of about  $950 \text{ m}^2/\text{g}$ . This material has been pyrolysed under Argon up to  $1000^\circ\text{C}$ . Conversion into a silicon oxycarbide glass has been followed by X-ray diffraction. The organised structure can be retained until  $800^\circ\text{C}$ . Further characterisations were performed by  $^{29}\text{Si}$  MAS NMR,  $^{13}\text{C}$  CP MAS NMR and  $\text{N}_2$  adsorption–desorption experiments to follow the structural changes occurring during the pyrolysis.

© 2004 Elsevier Ltd. All rights reserved.

**Keywords:** Periodic mesoporous organosilica; Sol–gel process; Pyrolysis; Porous glasses

## 1. Introduction

After the important discovery of ordered mesoporous silica in 1992 synthesised from inorganic precursors and amphiphilic molecules via a self-assembly process,<sup>1</sup> another class of materials emerged with the introduction of organic groups covalently bonded to the silica framework.<sup>2</sup> In a first step, organotrialkoxysilanes ( $\text{X}(\text{OR})_3$ ) were combined with tetraalkoxysilane to yield organically modified porous silica in a one-pot synthesis. In that case, the organic functions are pendant groups at the surface of the pores. A large range of alkoxy silanes and surfactants have been used to develop a great variety of functionalised silica with controlled pore structures.

In 1999, three research groups have simultaneously published a new class of material called periodic mesoporous organosilicas (PMOs)<sup>3–9</sup> based on bis-silylated precursors,  $(\text{RO})_3\text{Si-X-Si}(\text{OR})_3$ . They are true hybrid materials in

which the organic groups X are part of the framework. A large range of groups has been used among which  $-\text{CH}_2-$ ,<sup>3</sup>  $-\text{CH}_2-\text{CH}_2-$ ,<sup>4–7</sup>  $-\text{CH}=\text{CH}-$ ,<sup>8</sup> benzene.<sup>9,10</sup> The co-existence of Si–O and Si–C bonds makes them very suitable as precursors for porous silicon oxycarbide glasses. Previous studies on sol–gel-derived SiCO glasses have demonstrated the unique high temperature properties of these materials in terms of mechanical strength<sup>11</sup> and chemical durability.<sup>12</sup> Additionally, if these materials can exhibit a periodic porous network, then they can find applications as filters, catalysts or membranes for severe operating conditions.

Recently, we have demonstrated that PMOs obtained from bis(triethoxysilyl)ethane (BTM:  $(\text{OEt})_3\text{Si}-\text{CH}_2-\text{CH}_2-\text{Si}(\text{OEt})_3$ ) and bis(trimethoxysilyl)ethane (BTME:  $(\text{OMe})_3\text{Si}-\text{CH}_2-\text{CH}_2-\text{Si}(\text{OMe})_3$ ) present 2D-hexagonal or 3D-cubic structures, respectively.<sup>13</sup> The 2D-hexagonal structure is based on a packing of cylindrical micelles whereas the cubic one with a  $Pm\bar{3}n$  space group is characterised by a three-dimensional porous network based on the packing of spherical micelles. While the

\* Corresponding author. Tel.: +33 1 44 27 40 75; fax: +33 1 44 27 47 69.  
E-mail address: [fb@ccr.jussieu.fr](mailto:fb@ccr.jussieu.fr) (F. Babonneau).

2D-hexagonal structure collapses after pyrolysis at 800 °C under argon, the cubic structure is retained up to 1000 °C, leading to a SiCO glass with a large surface area of 730 m<sup>2</sup>/g.<sup>14</sup> Hence, the presence of a highly interconnected porous network in the starting PMO seems to be a key parameter to retain a large porosity in the final SiCO glass. Indeed, the cubic *Pm3n* structure has already been reported to be more robust towards heat treatment under air than the hexagonal structure.<sup>15</sup> However, we have also shown that the SiCO glass obtained from BTME still contains a free carbon phase (12 wt.%) that can be detrimental for high temperature properties. Hence, in order to decrease the carbon ratio in the final material, we have carried out an investigation on PMOs prepared from 1,2-bis(triethoxysilyl)-methane (BTM: (OEt)<sub>3</sub>Si–CH<sub>2</sub>–Si(OEt)<sub>3</sub>). In that case, the C/Si molar ratio is reduced to 1 compared to 2 for PMOs derived from BTME or BTEE. In a first part, we have investigated different synthetic parameters to see whether various porous structures and more specifically cubic ones, could be obtained. In a second part, the conversion of the PMOs into SiCO glasses was characterised combining X-ray diffraction with solid-state NMR and porosity measurements.

## 2. Experimental section

### 2.1. Chemicals

1,2-Bis(triethoxysilyl)-methane (BTM) was obtained from Gelest. Hexadecyltrimethylammonium chloride (C<sub>16</sub>TAC) (25 wt.% in water), sodium hydroxide (NaOH), and ethanol (99.5%) from Aldrich were used as received.

### 2.2. Synthesis

BTM was hydrolysed and condensed in the presence of C<sub>16</sub>TAC surfactant to yield methane-containing PMOs. Samples were prepared according to previously published conditions with slight modifications.<sup>3</sup> In a typical experiment, C<sub>16</sub>TAC was added to a mixture of BTM, NaOH and deionised water. The white suspension immediately formed was let under vigorous stirring at room temperature during 24 h and then kept at 90 °C for 48 h without stirring. After less than 1 h, the suspension precipitated. The latter was filtered off after cooling, washed twice with water and then dried at 100 °C overnight. The surfactant was removed by stirring under reflux for 18 h, 1.0 g of as-synthesised product in 100 ml of ethanol and 3 ml of a 36% HCl aqueous solution. The filtered sample was washed twice with ethanol and then dried at 80 °C overnight. The samples were pyrolysed under Argon in a tubular furnace at 200, 400, 600, 800 and 1000 °C with a heating rate of 5 °/min, and a final plateau of 2 h.

### 2.3. Characterisation

X-ray diffraction (XRD) patterns were recorded with a Bruker D8 X-ray diffractometer ( $\lambda = 1.54 \text{ \AA}$ ) or on the D43 beamline at the French synchrotron (LURE, Orsay) ( $\lambda = 1.447 \text{ \AA}$ ). <sup>29</sup>Si magic angle spinning (MAS) NMR spectra and <sup>13</sup>C cross polarisation (CP) MAS NMR spectra were recorded with a Bruker AVANCE 300 spectrometer at 59.62 MHz for <sup>29</sup>Si and 75.47 MHz for <sup>13</sup>C using 7 mm rotor spinning at 4 kHz. Scanning electron micrographs (SEM) were obtained with a Cambridge Stereoscan 120 microscope at an acceleration voltage of 10 kV. Transmission electron micrographs (TEM) were recorded with a JEOL JEM 100 cx II microscope at an acceleration voltage of 93 or 120 kV. The N<sub>2</sub> adsorption–desorption isotherms were measured at 77 K using a Micromeritics ASAP 2010 surface analyser. Elemental analyses were carried out by the Service Central d'Analyse, Vernaison, France.

## 3. Results and discussion

### 3.1. Effects of the synthesis conditions on the ordering of the as-prepared PMOs

After some attempts to synthesise PMOs under acidic conditions that result in no ordering, we have restricted our investigation to basic conditions using NaOH as catalyst. Table 1 summarised the range of experimental conditions that were tested.

#### 3.1.1. Effect of the pH

The basicity of the reaction mixture is an important factor that influences the degree of structural ordering and the yield of the self-assembly reaction. Three samples have been prepared at pH values of 12.7 (sample 1), 13.4 (sample 2) and 13.9 (sample 3). First, one can notice that the yield largely decreases by increasing the pH. This can be due to the better solubility of the silicate species at high pH, which prevents condensation reactions. Indeed, no suspension is observed at this highest pH at room temperature and the XRD pattern obtained on the small amount of precipitate recovered after treatment at 90 °C (Fig. 1a) shows almost no ordering. On the contrary, at lower pH values, the yield is much higher (70–80%) and the XRD patterns present a peak around  $2\theta = 1.70^\circ$ . The best ordering is observed for sample 2 prepared at pH 13.4. The corresponding pattern can be assigned to a 2D-hexagonal phase, even if no higher order peaks can be clearly distinguished. However, a better resolved pattern recorded with a synchrotron radiation shows one main peak at  $2\theta = 1.57^\circ$  and two weak peaks at  $2\theta = 2.73^\circ$  and  $2.89^\circ$  (Fig. 2a), which allows to calculate an hexagonal cell parameter,  $a = 6.1 \text{ nm}$ . Similar patterns have already been reported in the literature.<sup>3</sup> The corresponding TEM image shown in Fig. 2b confirms the well-ordered hexagonal structure of the sample.

Table 1  
List of samples with the corresponding synthesis and structural parameters

Sample	Molar composition (with respect to BTM)		pH	Post-treatment	Yield (%) <sup>b</sup>	DRX <sup>c</sup>	S <sub>BET</sub> (m <sup>2</sup> /g)
	C <sub>16</sub> TAC <sup>a</sup>	H <sub>2</sub> O					
1	0.12	114	13.9	24 h, RT/48 h, 90 °C	22	No	
2	0.12 (0.11)	114	13.4	24 h, RT/48 h, 90 °C	72	S	950
3	0.12	114	12.7	24 h, RT/48 h, 90 °C	83	X	730
4	0.25 (0.22)	114	13.4	24 h, RT/48 h, 90 °C	70	X	1040
5	0.5 (0.28)	114	13.4	24 h, RT/48 h, 90 °C	77	x	
6	0.75 (0.31)	114	13.4	24 h, RT/48 h, 90 °C	73	x	
7	1.0 (0.30)	114	13.4	24 h, RT/48 h, 90 °C	78	x	
8	0.12	114	13.4	24 h, RT/24 h, 90 °C	67	S	770
9	0.12	114	13.4	24 h, RT	35	x	
10	0.12	114	13.4	48 h, 90 °C	65	X	950
11	0.12	228	13.4	24 h, RT/48 h, 90 °C	49	X	
12	0.12	342	13.4	24 h, RT/48 h, 90 °C	25	x	

<sup>a</sup> The value corresponds to the ratio introduced in solution. The value extracted from elemental analysis performed on the dried precipitate is indicated in parentheses.

<sup>b</sup> The yield is defined as the amount of powder collected after precipitation by comparison with the theoretical one.

<sup>c</sup> Degree of ordering detected by XRD: S, good; X, medium; x, poor order.

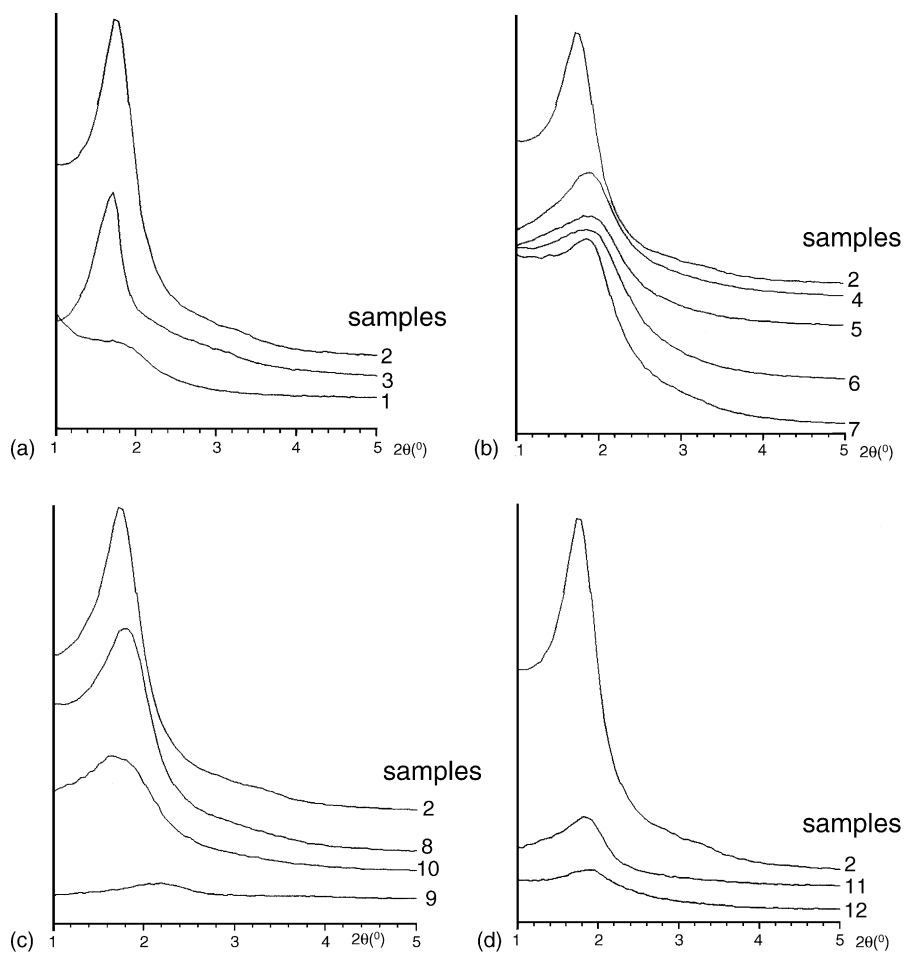


Fig. 1. XRD patterns of as-prepared BTM-derived samples after surfactant extraction. (a) Influence of the pH; (b) influence of the C<sub>16</sub>TAC/BTM molar ratio; (c) influence of the post-treatment and (d) influence of the concentration. The numbers for each pattern correspond to the samples listed in Table 1.

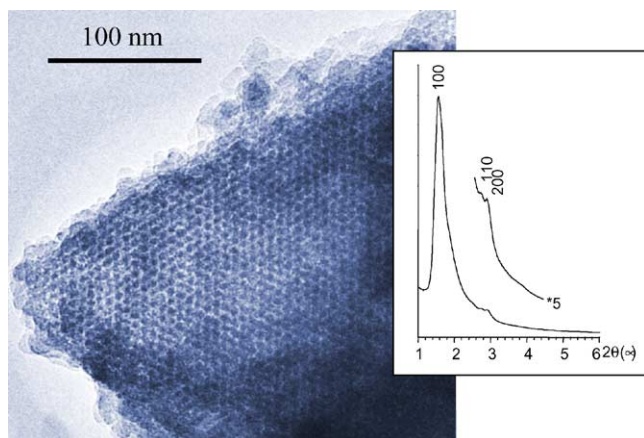


Fig. 2. (a) XRD pattern recorded with the synchrotron radiation and (b) TEM image characteristic of sample 2.

### 3.1.2. Effect of the $C_{16}TAC/BTM$ molar ratio

Samples have been prepared with various  $R = C_{16}TAC/BTM$  molar ratios (Table 1, samples 2, 4–7). Interestingly, elemental analysis performed on these samples shows that above 0.25, only part of the surfactant is incorporated in the material. The maximum amount seems to level out around 0.30 even if the starting  $R$  value is as high as 1. Whatever the  $R$  value, the yield remains almost constant around 70–80%, but with a decrease in the ordering when  $R$  increases (Fig. 1b). This behaviour was already reported for the BTME-derived samples.<sup>7</sup>

### 3.1.3. Effect of the post-treatment

The standard curing procedure (24 h at room temperature and 48 h at 90 °C) has been changed to estimate whether these two steps had an influence on the extent of ordering (Table 1, samples 2, 8–10). Suppression of the step at 90 °C (sample 9) results in a very low yield and a poorly ordered sample (Fig. 1c). Suppression of the step at room temperature is less dramatic for the structure (sample 10); however, the combination of both steps yields to the best ordering, with almost no difference between 24 or 48 h at 90 °C.

### 3.1.4. Effect of the concentration

Samples have been prepared with different concentrations of reactants in the aqueous solution (Table 1, samples 2, 11, 12). The yield greatly decreases with dilution, and this is also affecting the extent of ordering (Fig. 1d).

### 3.1.5. Conclusion

This study allows to define the synthesis parameters that seem to be the most appropriate to obtain ordered BTM-derived samples. The following composition was obtained:  $BTM:C_{16}TAC:NaOH:H_2O = 1:0.12:0.5:114$  (molar ratio). However, one can notice that even for this optimised composition, the XRD peaks are much broader—about seven

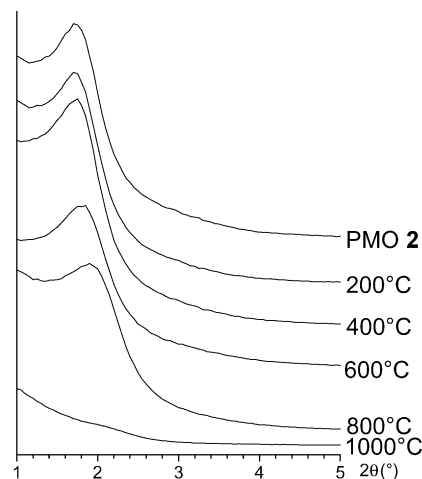


Fig. 3. XRD patterns of BTM-derived sample (#2), calcined at 200, 400, 600, 800 and 1000 °C.

times in  $2\theta$ —than for the BTEE-derived sample.<sup>13</sup> This suggests that it seems rather difficult to obtain a well-ordered structure with BTM. Indeed, very few papers have been published with this precursor compared to BTEE or BTME that have been much more investigated. Also, only hexagonal phases have been obtained, another difference with respect to the BTME-derived samples for which cubic as well as 3D-hexagonal phases have been reported.<sup>7</sup> Nevertheless, the specific surface area of the BTM-derived PMO can reach almost 1000 m<sup>2</sup>/g, which is a good characteristic for a mesoporous material.

### 3.2. Study of the thermal stability

The best ordered BTM-derived PMO (sample 2) was pyrolysed under Argon up to 1000 °C. The corresponding XRD patterns are presented in Fig. 3. XRD peaks are observed until 800 °C; at 1000 °C, the structure has finally collapsed. With increasing temperature, the peaks slightly shift to greater  $2\theta$  values, especially for  $T > 600$  °C indicating a contraction of the cell parameter (−9% at 800 °C). The peaks are also broadening with temperature, which might indicate a decrease in the long-range mesoscopic order of the sample.

N<sub>2</sub> adsorption–desorption isotherms were recorded on each sample, and the results data are summarised in Table 2. Up to 400 °C, the porosity parameters remain almost constant with a large surface area around 960–980 m<sup>2</sup>/g, a pore volume determined with the BJH model around 1.1 cm<sup>3</sup>/g and pore size around 4 nm. Interestingly, up until 800 °C, the surface area decreases to a small extent (790 m<sup>2</sup>/g). The pore volume drops to 0.65 cm<sup>3</sup>/g at 800 °C, and down to 0.20 cm<sup>3</sup>/g at 1000 °C. On the other hand, the pore diameter remains constant (4 nm) until 800 °C, and decreases to 2 nm at 1000 °C. The large changes observed at 1000 °C are in good agreement with the total collapse of the structure observed by X-ray diffraction.

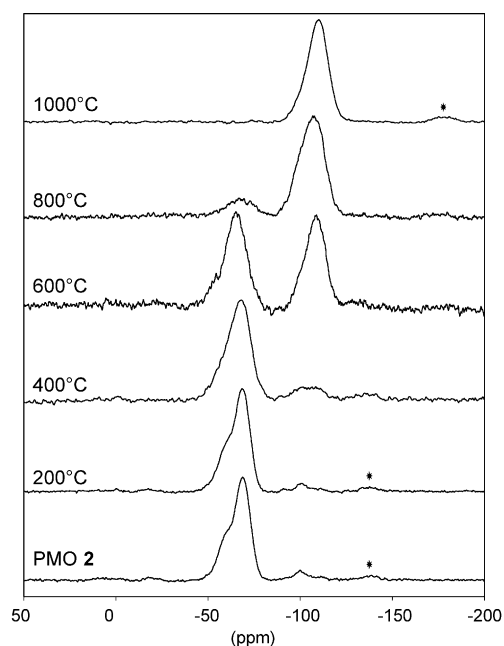


Fig. 4.  $^{29}\text{Si}$  MAS NMR spectra of BTM-derived sample (#2), calcined at 200, 400, 600, 800 and 1000 °C. Asterisk (\*) corresponds to spinning side bands.

$^{29}\text{Si}$  NMR experiments were recorded on the different pyrolysis intermediates to follow the changes of the local environment of Si sites during the ceramisation process (Fig. 4). The spectrum of the PMO sample displays a main broad peak around  $-67$  ppm characteristic of  $T_3$  units:  $(-\text{O})_3\text{Si}(\text{C})-$  showing that the Si–C bonds survived to the synthesis procedure. The dissymmetry of the peak at low field is due to the presence of a peak around  $-60$  ppm due to  $T_2$  units with one terminal Si–OH group. However, the  $T_2/T_3$  molar ratio (1:2) shows a rather high degree of condensation for the organosilica framework. The presence of a weak signal at about  $-100$  ppm which is characteristic of  $Q$  units:  $\text{Si}(\text{O})_4-$  indicates that the cleavage of some Si–C bonds occurs during the synthesis course, but to a low extent (3% of total Si atoms). At 200 °C, the environment of the Si sites does not change. As the treatment temperature increases up to 400 °C, a continuous conversion of the  $T$  units into  $Q$  units occurs. The  $T/Q$  ratio varies from 15:85 at 400 °C, to 45:55 at 600 °C, 85:15 at 800 °C and finally 100:0 at 1000 °C. At this temperature, the

Table 2

Results extracted from  $\text{N}_2$  adsorption–desorption isotherms and XRD patterns obtained on the BTM-derived sample pyrolysed at various temperatures

	$\text{N}_2$ adsorption data			XRD data	
	$S_{\text{BET}}$ ( $\text{m}^2/\text{g}$ )	$V_{\text{BJH}}$ ( $\text{cm}^3/\text{g}$ )	$\phi$ (Å)	$2\theta$ ( $^\circ$ )/ $d_{100}$ (nm)	$a$ (nm)
PMO	980	1.10	40	1.72/5.13	5.92
200 °C	980	1.10	40	1.72/5.13	5.92
400 °C	960	1.05	40	1.75/5.03	5.81
600 °C	840	1.00	40	1.81/4.87	5.62
800 °C	790	0.65	39	1.93/4.57	5.28
1000 °C	210	0.20	–	–	–

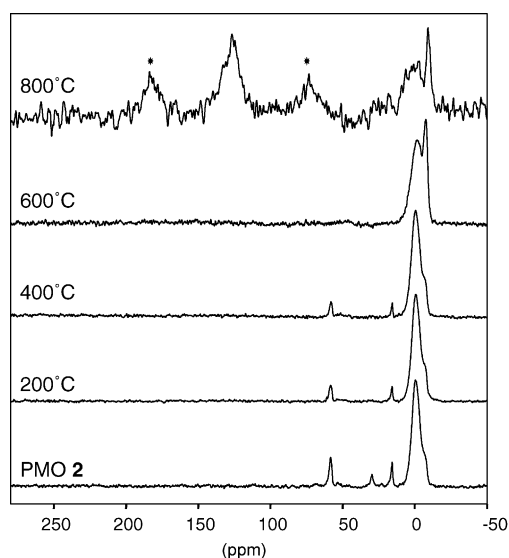


Fig. 5.  $^{13}\text{C}$  CP MAS NMR spectra of BTM-derived sample (#2), calcined at 200, 400, 600, 800 and 1000 °C.

Si-containing phase can be described as a pure amorphous silica phase, with no residual Si–C bonds.

All the samples were also analysed by  $^{13}\text{C}$  CP MAS NMR (Fig. 5). The spectrum of the PMO sample shows a main peak at  $-0.6$  ppm, with a shoulder around  $-6.4$  ppm. The use of a modified version of the CP sequence, called inversion recovery cross polarisation (IRCP)<sup>16</sup> allows us to assign the two peaks to Si– $\text{CH}_2$ –Si and Si– $\text{CH}_3$  groups, respectively. The presence of this last peak confirms that a part of the Si–C bonds has been cleaved during the synthesis (supposedly through hydrolysis), in good agreement with the presence of  $Q$  units in the  $^{29}\text{Si}$  MAS NMR spectrum. The two peaks at 15.7 and 58.3 ppm are due to ethoxy groups, which have been certainly introduced during the surfactant extraction step that uses ethanol as solvent. The weak peak around 29.6 ppm is due to a small amount of residual surfactant that can be eliminated after an additional solvent extraction step. Increasing the temperature up to 400 °C did not cause major changes, except the total disappearance of the surfactant peak. At 600 °C, the ethoxy peaks have now disappeared, but the major change is the increase of a sharp peak at  $-7.6$  ppm due to Si– $\text{CH}_3$  groups and the broadening of the peak previously assigned to Si– $\text{CH}_2$ –Si groups. These changes occur simultaneously with the large increase of  $Q$  units in the  $^{29}\text{Si}$  MAS NMR spectrum. They can thus be viewed as the cleavage of Si– $\text{CH}_2$ –Si bonds to give Si– $\text{CH}_3$  groups and new Si–O bonds. This reaction could be assisted by the presence of Si–OH group as already suggested by Ozin and co-workers.<sup>3</sup> At 800 °C, the poor signal/noise ratio of the spectrum indicates a large decrease of the proton content which prevents a good efficiency of the magnetisation transfer between the protons and the  $^{13}\text{C}$  spins. In the aliphatic C range, the sharp peak due to Si– $\text{CH}_3$  groups is still present in agreement with the good temperature resistance of the Si–C bond in such groups. The component at lower field is broadening, suggesting the presence of a

distribution of C environment, certainly due to dehydrogenation reactions leading to the formation of  $\text{CH}_{2-x}(\text{Si})_{2+x}$  sites with  $x$  increasing from 0 to 2. Despite the dehydrogenation reactions, the major change is the appearance of aromatic signals around 130 ppm, characteristic of the formation of a free carbon phase. This is in perfect agreement with the  $^{29}\text{Si}$  MAS NMR spectrum that does not show any longer the presence of Si–C bonds. The resulting glass can be described as an amorphous  $\text{SiO}_2$  phase in which a free C phase is embedded.

#### 4. Conclusion

PMOs have been prepared from bis(triethoxysilyl)methane and cetyltrimethylammonium chloride varying a large number of synthetic parameters (pH, concentration of surfactant, dilution, curing treatment) to optimise the extent of ordering of the porous phase. Only 2D-hexagonal phases were obtained with surface areas as high as  $980 \text{ m}^2/\text{g}$ . Pyrolysis under argon retain an ordered structure up to  $800^\circ\text{C}$ , with a large surface area of  $790 \text{ m}^2/\text{g}$ . At this temperature, the silica-based framework still contains some Si–C bonds, but most of the C is now present in a free C phase. By  $1000^\circ\text{C}$ , the Si–C bonds are totally cleaved and the ordered structure has collapsed.

This behaviour is very similar to what has been already found for 2D-hexagonal PMOs prepared from bis(triethoxysilyl)ethane, and different from the great temperature resistance of the  $Pm\bar{3}n$  cubic structure obtained from bis(trimethoxysilyl)ethane that resists to pyrolysis temperatures as high as  $1000^\circ\text{C}$ , leading to a true silicon oxycarbide porous phase.

In conclusion, it seems very difficult to convert a PMO sample with a 2D-hexagonal structure into a SiCO glass with ordered porosity. By  $1000^\circ\text{C}$ , the structure collapses with a complete cleavage of the Si–C bonds. Up to now, the only success to produce a porous SiCO glass was obtained starting from a PMO with a cubic structure.

#### Acknowledgements

Dominique Durand from LURE (Orsay, France) and Jocelyne Maquet from LCMC (Paris, France) are greatly acknowledged for their help in the XRD and NMR measurements.

#### References

1. Kresge, C. T., Leonowicz, M. E., Roth, W. J., Vartuli, J. C. and Beck, J. S., *Nature*, 1992, **359**, 710.
2. Stein, A., Melde, B. J. and Schroden, R. C., *Adv. Mater.*, 2000, **12**, 1403, and references herein.
3. Asefa, T., MacLachlan, M. J., Grondey, H., Coombs, N. and Ozin, G. A., *Angew Chem. Int. Ed.*, 2000, **39**, 1808.
4. Inagaki, S., Guan, S., Fukushima, Y., Ohsuna, T. and Terasaki, O., *J. Am. Chem. Soc.*, 1999, **121**, 9611.
5. Melde, B. J., Holland, B. V. T., Blanford, C. F. and Stein, A., *Chem. Mater.*, 1999, **11**, 3302.
6. (a) Guan, S., Inagaki, S., Ohsuna, T. and Terasaki, O., *J. Am. Chem. Soc.*, 2000, **122**, 5660;  
(b) Sayari, A., Hamoudi, S., Yang, Y., Moudrakovski, I. L. and Ripmeester, J., *Chem. Mater.*, 2000, **12**, 3857.
7. Guan, S., Inagaki, S., Ohsuna, T. and Terasaki, O., *Micr. Meso. Mater.*, 2001, **44/45**, 165.
8. Asefa, T., MacLachlan, M. J., Coombs, N. and Ozin, G. A., *Nature*, 1999, **402**, 867.
9. Yoshina-Ishii, C., Asefa, T., Coombs, N., MacLachlan, M. J. and Ozin, G. A., *Chem. Commun.*, 1999, 2539.
10. Inagaki, S., Guan, S., Ohsuna, T. and Terasaki, O., *Nature*, 2002, **416**, 304.
11. Rouxel, T., Massouras, G. and Soraru, G. D., *J. Sol-Gel Sci. Technol.*, 1999, **14**, 87.
12. Soraru, G. D., Modena, S., Guadagnino, E., Colombo, P., Egan, J. and Pantano, C., *J. Am. Ceram. Soc.*, 2002, **85**, 1529.
13. Toury, B., Blum, R., Goletto, V., Babonneau, F., manuscript in preparation.
14. Blum, R., Goletto, V., Toury, B. and Babonneau, F., *Mat. Res. Soc. Symp. Proc.*, 2003, **775**, 77.
15. Goletto, V., Impéror, M. and Babonneau, F., *Proceedings of the 13th International Zeolite Conference, Montpellier (2001) in Studies in Surface Science and Catalysis, Vol 35*, ed. A. Galarneau, F. Di Renzo, F. Fajula and J. Védrine. Elsevier, 2001, p. 150.
16. Gualandris, V., Hourlier-Bahloul, D. and Babonneau, F., *J. Sol-Gel Sci. Technol.*, 1999, **14**, 39.